Journal of Applied Mechanics and Technical Physics, Vol. 43, No. 6, pp. 854–860, 2002

EFFECT OF DYNAMIC PREHISTORY ON AERODYNAMICS OF A LAMINAR SEPARATED FLOW IN A CHANNEL BEHIND A RECTANGULAR BACKWARD-FACING STEP

S. R. Batenko and V. I. Terekhov

UDC 532.517.2 + 532.526

The effect of dynamic prehistory of the flow and the channel-expansion ratio on aerodynamics of a steady separated laminar flow behind a rectangular backward-facing step located in a plane-parallel channel is numerically studied. It is shown that the boundary layer upstream of the flow separation exerts a strong effect on flow characteristics behind the step. A decrease in the boundary-layer thickness in the cross section of the step leads to a decrease in the separation-region length, and an increase in the channel-expansion ratio with a fixed initial boundary-layer thickness and Reynolds number leads to an increase in the separation-region length.

The problem of the flow around a backward-facing step is the classical problem of gas dynamics and is of both scientific and practical interest. First, because of the fixed position of the separation point, the simplest case of separated flow seems to be observed in this case; second, flows under these conditions are frequently encountered in nature and engineering.

In studying separated flows, the main attention is traditionally paid to the turbulent regime because of its abundance in nature. Nevertheless, laminar flows are also of significant interest, which is primarily related to optimization of constructions of compact heat exchangers.

Laminar separated flows were considered by many researchers. Goldstein et al. [1] studied the laminar–turbulent transition in a separated boundary layer behind a rectangular backward-facing step in a channel of large width and height as compared to the step. Based on the results of smoke visualization and hot-wire measurements, criteria of existence of the laminar regime within the entire separated flow region were derived. Experimental data on the dependence of the separation-region length r on the Reynolds number $\mathrm{Re}_s = u_s s/v$ and the boundary-layer displacement thickness δ^* in the cross section where the step was located were also obtained. Using these data, Goldstein et al. [1] significantly refined the formula proposed by Cramer [2], where the separation-region length depends linearly on Re_{δ^*}, and the coefficients are proportional to the displacement thickness δ^*.

Sinha et al. [3] considered the flow around rectangular backward-facing steps of various heights, which were located in a channel. The experiments were performed in a low-turbulent flow with the Reynolds number varied within $10^2 < \mathrm{Re}_s < 1.5 \cdot 10^4$. A dependence $r(\mathrm{Re}_s)$ was obtained. According to the data of [3], the separated boundary layer remains laminar up to $\mathrm{Re}_s \approx 820$, and the separation-region length is directly proportional to the Reynolds number. For $\mathrm{Re}_s \approx 820$, the separation-region length is maximum: $r \approx 21s$ (s is the step height). With further increase in the Reynolds numbers, a laminar–turbulent transition occurs in the separated boundary layer; as a consequence, the separation-region length gradually decreases to $r \approx 6s$. This value corresponds to a steady turbulent flow regime with $\mathrm{Re}_s > 8 \cdot 10^3$.

Armaly et al. [4] performed a similar study; in contrast to [1, 3], the authors used a moderate-height channel (twice the step height only). Precision hot-wire measurements were performed within the range of Reynolds numbers $70 < \mathrm{Re}_s < 8 \cdot 10^3$. The experiment showed that, in addition to the main region of the separated flow, there are two more regions of secondary separation of the flow located on the upper and lower walls within certain ranges

Kutateladze Institute of Thermal Physics, Siberian Division, Russian Academy of Sciences, Novosibirsk 630090. Translated from Prikladnaya Mekhanika i Tekhnicheskaya Fizika, Vol. 43, No. 6, pp. 84–92, November–December, 2002. Original article submitted March 5, 2002.

 0021-8944/02/4306-0854 $27.00

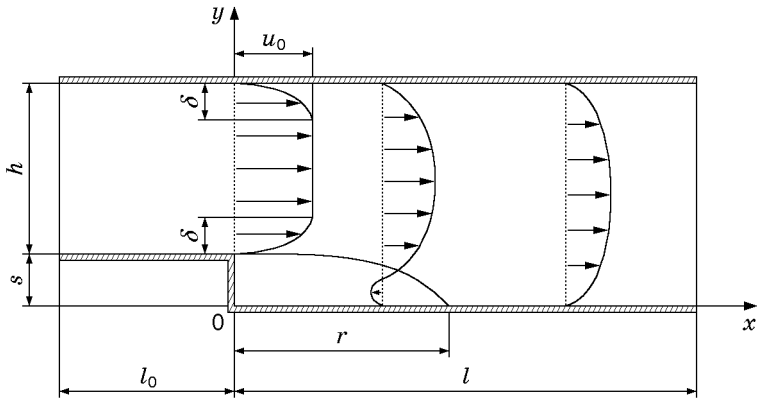

Fig. 1. Computational domain and flow pattern.

of Re_s. The laminar–turbulent transition begins at $\mathrm{Re}_s \approx 1200$, and the maximum length of the primary separation region is $r \approx 17.5s$. The turbulent regime is established for $\mathrm{Re}_s \approx 6600$. It corresponds to a separation region of length $r \approx 8s$. Numerical simulation of a two-dimensional laminar flow in the channel of the above-mentioned geometry was also performed in [4]. Good agreement with experimental data was obtained for Reynolds numbers up to $\mathrm{Re}_s \approx 450$. For $\mathrm{Re}_s > 450$, significant disagreement is observed, which is attributed to the three-dimensional character of the flow in [4].

Aung [5] experimentally studied the temperature field in the case of a laminar flow around a rectangular backward-facing step. It is shown, in particular, that the separation-region length in a laminar flow depends not only on the Reynolds number Re_s but also on the displacement thickness δ^*. Numerical simulation of aerodynamics and heat transfer for a similar geometry was performed in [6], which is a continuation of [5], but the dependence of the separation-region length r on the displacement thickness δ^* and Reynolds number Re_s found in [6] turned out to be complicated, nonmonotonic, and difficult for analysis. In addition, the results of several independent investigations presented in one figure in [6] showed that there is a large scatter of data on the separation-region length depending on the Reynolds number in laminar flows. This is explained by the difference in physical conditions, though the influence of the governing factors remains not clear yet.

The objective of the present study is a numerical analysis of the influence of the boundary-layer thickness δ in the cross section where the step is located on dynamic characteristics of the flow behind the step. The varied parameters in calculations were the Reynolds number ($\mathrm{Re}_s = 10$–400), boundary-layer thickness (from the minimum to the maximum possible value $\delta_{\max} = 0.5h$), and the channel-expansion ratio $ER = (h + s)/h = 1.17$, 1.33, and 2.00.

1. Formulation of the Problem, Numerical Model, and Boundary Conditions. We consider a steady laminar two-dimensional viscous incompressible liquid flow with constant properties in a plane-parallel channel with sudden expansion in the form of a rectangular backward-facing step. Figure 1 schematically shows the computational domain, velocity profiles in various cross sections of the channel, and separated flow region. The origin is located in the bottom left corner of the channel and coincides with the step base. The reference scales of length and velocity are the step height s and the mean-mass velocity in the cross section where the step is located u_s; they are used to normalize all linear dimensions and velocities.

A symmetric rectangular velocity profile with the boundary-layer thickness tending to zero is set at the channel entrance. At the initial section of length l_0, the velocity profile deforms, and boundary layers start to grow on the upper and lower walls of the channel. The shape of the velocity profile in the cross section where the step is located is affected by the flow velocity u_s (or the Reynolds number Re_s), the length of the initial section l_0, and the channel-expansion ratio $ER = (h + s)/h$. Combinations of the above parameters are numerous; therefore, we consider a simpler case, where the upper and lower boundary layers in the cross section where the step is located have an identical thickness δ. This parameter is assumed to be the most important for understanding the versatile data accumulated on the separation-region length as a function of the Reynolds number.

A symmetric velocity profile is set in the cross section where the step is located. It is prescribed by the expression

$$u(y) = \begin{cases} (y_1 - y)(y - y_1 - 2\delta)/\delta^2, & y_1 < y < y_1 + \delta, \\ u_0, & y_1 + \delta \leqslant y \leqslant y_2 - \delta, \\ (y_2 - y)(y - y_2 + 2\delta)/\delta^2, & y_2 - \delta < y < y_2, \end{cases} \tag{1}$$

where y_1 and y_2 are the coordinates of the top of the step and the upper wall of the channel (Fig. 1). Thus, the velocity has a constant value in the central region $[u_0 = (1 - 2\delta/(3h))^{-1}]$ and follows a parabolic law in boundary layers.

The channel flow was numerically simulated by an iterative solution of unsteady Navier–Stokes equations written for an incompressible viscous liquid with constant properties in the variables "stream function–vortex":

$$\frac{\partial \xi}{\partial t} + \frac{\partial u\xi}{\partial x} + \frac{\partial v\xi}{\partial y} = \frac{1}{\mathrm{Re}_s}\Big(\frac{\partial^2 \xi}{\partial x^2} + \frac{\partial^2 \xi}{\partial y^2}\Big), \qquad \frac{\partial^2 \psi}{\partial x^2} + \frac{\partial^2 \psi}{\partial y^2} = \xi,$$

$$u = \frac{\partial \psi}{\partial y}, \qquad v = -\frac{\partial \psi}{\partial x}.$$

It is also convenient to write the equation for the stream function in an unsteady form by adding a dummy derivative with respect to time: $\partial\psi/\partial t = \partial^2\psi/\partial x^2 + \partial^2\psi/\partial y^2 - \xi$. This trick is acceptable in the above-described formulation of the problem, since we seek a steady solution, and the derivative in time vanishes after all. The vortex-transfer equation remains unchanged. Finally, both equations have an unsteady character. Their steady solutions are found by the pseudotransient method by iterations in time. This is done using the implicit scheme of the method of alternating directions described in [7]:

$$\frac{f^{n+1/2} - f^n}{\delta t/2} + \Big(\frac{\delta u f}{\delta x}\Big)^{n+1/2} + \Big(\frac{\delta v f}{\delta y}\Big)^{n} - \alpha\Big(\frac{\delta^2 f}{\delta x^2}\Big)^{n+1/2} - \alpha\Big(\frac{\delta^2 f}{\delta y^2}\Big)^{n} = 0,$$

$$\frac{f^{n+1} - f^{n+1/2}}{\delta t/2} + \Big(\frac{\delta u f}{\delta x}\Big)^{n+1/2} + \Big(\frac{\delta v f}{\delta y}\Big)^{n+1} - \alpha\Big(\frac{\delta^2 f}{\delta x^2}\Big)^{n+1/2} - \alpha\Big(\frac{\delta^2 f}{\delta y^2}\Big)^{n+1} = 0.$$

Here n is the iteration number and δt is the time step. We have $f = \xi$ and $\alpha = 1/\mathrm{Re}_s$ in the vortex-transfer equation and $f = \psi$ and $\alpha = 1$ in the stream function equation; the sum of convective terms is substituted by ξ^n.

We used first-order upstream differences in steps of spatial variables for discretization of convective terms and second-order central differences for discretization of diffusion terms.

The no-slip conditions $u = 0$ and $v = 0$ are set on the walls; therefore, the stream function on them is constant: $\psi = \mathrm{const}$. Woods' condition is used for the vortex on the walls:

$$\xi_w + \frac{1}{2}\,\xi_{w+1} + 3\,\frac{\psi_w - \psi_{w+1}}{\Delta y^2} + O(\Delta y^2) = 0.$$

The velocity profile (1) is specified at the input boundary; and the stream function

$$\psi = \psi(y) = \int u(y')\,dy' + \mathrm{const}$$

and the vortex

$$\xi = \Delta\psi = \frac{\partial^2 \psi}{\partial y^2}$$

are rigorously defined there. Soft conditions are set at the output boundary:

$$\frac{\partial^2 \xi}{\partial x^2} = 0, \qquad \frac{\partial^2 \psi}{\partial x^2} = 0.$$

We introduce the following notation for local quantities that characterize friction and are used to analyze the results: all dimensionless quantities are marked by the tilde sign, and all quantities without this symbol are dimensional (except for the Reynolds number Re_s and friction coefficient $C_f/2$). The shear stress for the streamwise velocity is set by the expression

$$\tau = \mu\,\frac{\partial u}{\partial y} = \frac{\mu u_s}{s}\,\frac{\partial \tilde{u}}{\partial \tilde{y}}.$$

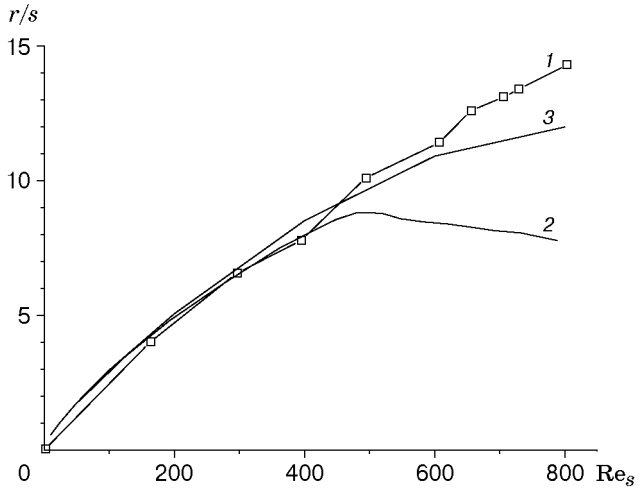

Fig. 2. Calculated and experimental dependences of the separation-region length r on the Reynolds number Re_s: points 1 refer to the experimental data of [4] and curves 2 and 3 show the calculated data of [4] and the present work, respectively.

From here, we obtain the expression for the friction coefficient on the lower wall of the channel:

$$\frac{C_f}{2} = \frac{\tau_w}{\rho u_s^2} = \frac{1}{\rho u_s^2}\,\frac{\mu u_s}{s}\,\frac{\partial \tilde{u}}{\partial \tilde{y}}\Big|_w = \frac{1}{\mathrm{Re}_s}\,\frac{\partial \tilde{u}}{\partial \tilde{y}}\Big|_w.$$

2. Testing of the Model. The applicability of the model was tested by a comparison with the experiment of Armaly et al. [4] who considered a laminar flow in a plane-parallel channel with sudden expansion in the form of a rectangular backward-facing step. The size of the computational domain relative to the step height s corresponded to the experimental values: the channel height at the initial section $h_0 = 1$ and the channel length $l_0 = 40$; after expansion, we had $h = 2$ and $l = 100$. The computational grid was uniform in each coordinate direction and had 561 and 101 nodes in the x and y directions, respectively. A velocity profile similar to (1) was set at the channel entrance, with a minimum boundary-layer thickness possible for this grid $\delta_0 = 0.02$.

The calculated and experimental results of [4] are plotted in Fig. 2. The point of flow reattachment was determined from the zero value of the friction coefficient on the lower wall of the channel in calculations and by hot-wire measurements of velocity near the wall in the experiment of [4]. It follows from Fig. 2 that the calculation results are in good agreement with the experimental data up to $\mathrm{Re}_s \approx 600$. The numerical experiment of [4] yields similar results, but good agreement between the calculation and experiment is observed up to $\mathrm{Re}_s \approx 450$. Apparently, this difference is caused by manifestation of the three-dimensional character of the flow and the beginning of the transitional regime.

3. Calculation Results. 3.1. *Effect of the Initial Boundary-Layer Thickness on Flow Aerodynamics behind the Step.* The flow in the channel behind the step was calculated for the following conditions: in dimensionless variables, the step height was $s = 1$, the channel height in the cross section where the step was located was $h = 6$, i.e., the expansion ratio was $ER = 1.17$, and the channel length behind the step was $l = 40$. The boundary-layer thickness in the cross section of the step was $\delta = 0.1$, 0.24, 0.5, 1.0, 2.0, and 3.0; in other words, the boundary layer varied from the superthin to the developed state. The Reynolds number varied from 10 to 400. Its maximum value corresponded to the laminar–turbulent transition region. The computational grid was uniform in each coordinate direction (201 and 351 nodes in the x and y directions, respectively).

The calculation results for the separation-region length are plotted in Fig. 3a and compared with experimental and calculated data of other authors borrowed from [6] in Fig. 3b. The reattachment point was determined by the position of the point with zero friction coefficient, as in the test calculation. It should be noted that the dependence $r(\mathrm{Re}_s)$ is close to linear. At the same time, it is seen from Fig. 3a that the boundary-layer thickness δ in the cross section where the step is located determines the slope of this line: the slope increases with increasing boundary-layer thickness. For high values of Re_s, a decrease in the relative boundary-layer thickness from 3.0 to 0.1 leads to more than a threefold decrease in the separation-region length.

In addition, it follows from Fig. 3b that almost all data available in the literature lie within the region between the lines calculated in the present work and corresponding to the initial boundary-layer thicknesses $\delta = 0.5$

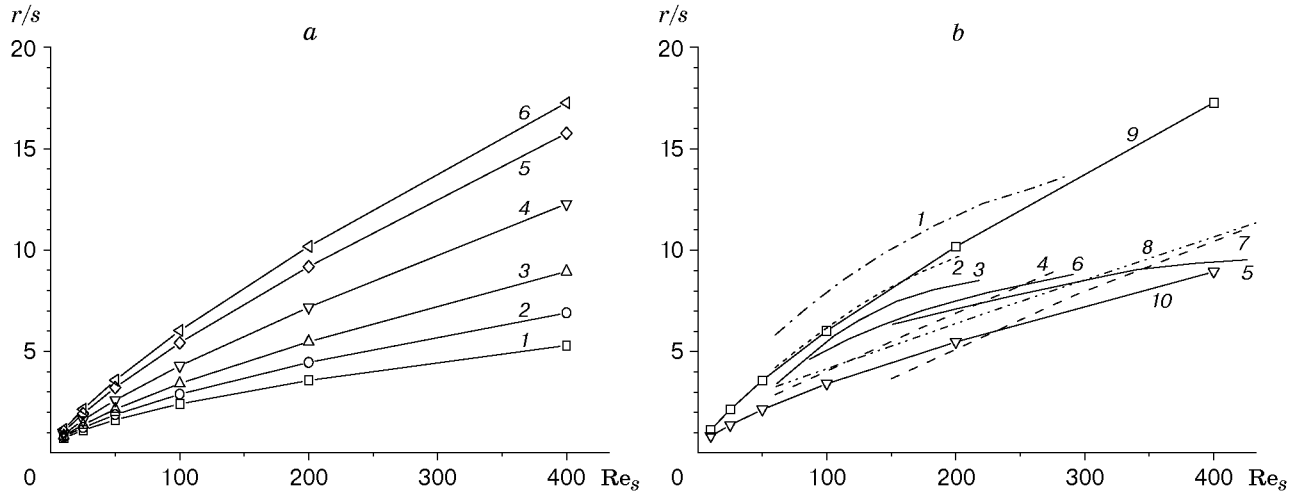

Fig. 3. Calculated dependence of the separation-region length r on the Reynolds number Re_s and initial thickness of the dynamic boundary layer δ for $ER = 1.17$: (a) data of the present work for $\delta = 0.1$ (1), 0.24 (2), 0.5 (3), 1.0 (4), 2.0 (5), and 3.0 (6); (b) results of other works cited in [6]: data of [8] (1), data of [9] (2), data of [6] for $s = 3.8$ (3), 6.4 (4), and 12.7 mm (5), data of [5] for $s = 6.4$ (6) and 2.7 mm (7), data of [1] (8), and data of the present work for $\delta = 3$ (9) and 0.5 (10).

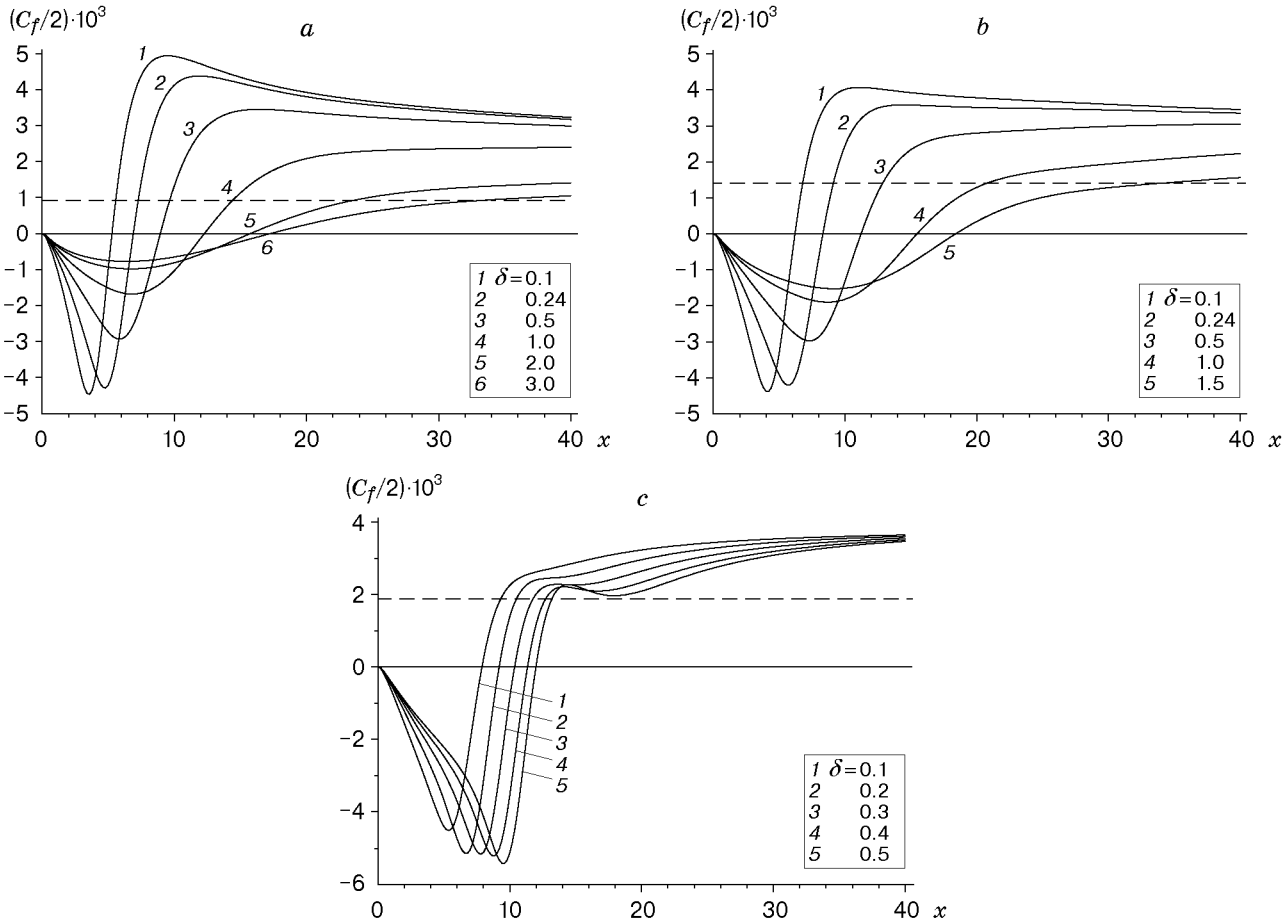

Fig. 4. Friction coefficient on the lower wall of the channel versus the initial boundary-layer thickness δ for $\mathrm{Re}_s = 400$ and $ER = 1.17$ (a), 1.33 (b), and 2 (c); the dashed curves show the values of the friction coefficient in a steady flow in the channel behind the reattachment point.

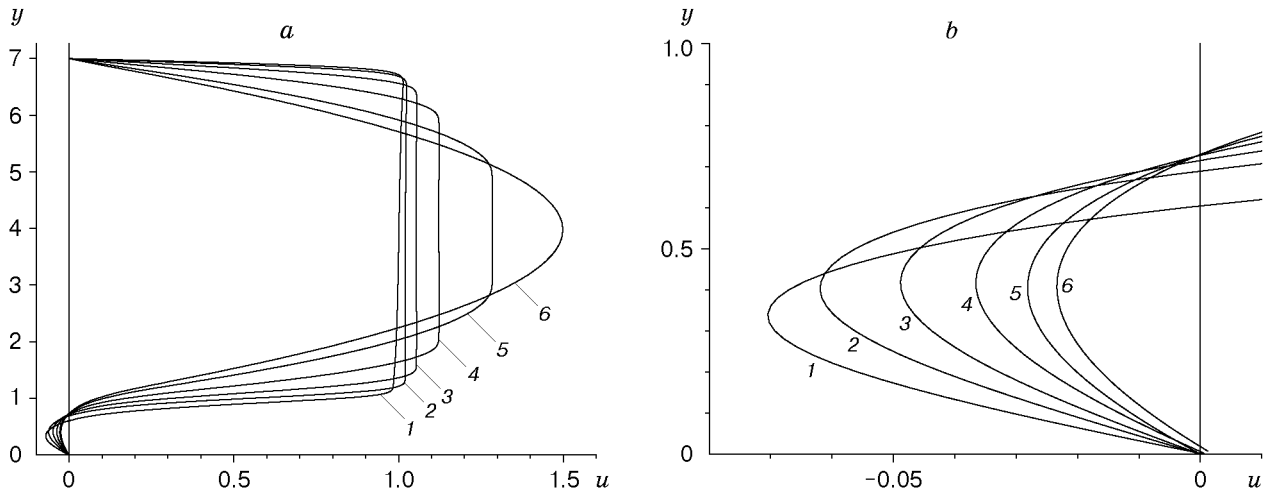

Fig. 5. (a) Full profiles of the streamwise velocity u for $x = 1.0$, $ER = 1.17$, and $\mathrm{Re}_s = 400$ and different initial boundary-layer thicknesses $\delta = 0.1$ (1), 0.24 (2), 0.5 (3), 1.0 (4), 2.0 (5), and 3.0 (6); (b) magnified image of the back flow region.

and 3.0. This indicates that one of the main parameters determining the scatter of reattachment-point coordinates is the boundary-layer thickness ahead of the separation point. It also follows from Fig. 3b that most known data belong to the region $\delta > 0.5$, which corresponds to real conditions of the experiments performed.

The calculated friction coefficient on the lower wall of the channel for $\mathrm{Re}_s = 400$ and various values of δ and ER are plotted in Fig. 4. The data in Fig. 4a are obtained for an expansion ratio $ER = 1.17$. As the initial boundary-layer thickness δ decreases, the maximum absolute value of the friction coefficient increases in the recirculation region where the flow-velocity direction is opposite to the main-flow velocity. The maximum value of the friction coefficient behind the flow-reattachment point also increases. Processing of the calculation data allows us to conclude that the absolute maximum value of the friction coefficient in the separation region can increase sixfold if the initial boundary-layer thickness δ decreases from 3.0 to 0.1.

The main reason for the strong influence of the boundary-layer thickness ahead of the separation point on friction in the separation region and the length of the latter is the decrease in the shear-layer thickness inside the separation region. This conclusion follows from the data plotted in Fig. 5, which shows the streamwise velocity profiles in the separation region ($x = 1$) for different boundary-layer thicknesses ahead of the step. For low values of δ, the velocity gradient is significantly higher both in the near-wall region and in the mixing layer than for high values of δ, which finally leads to an increase in shear stress and earlier reattachment of the boundary layer.

3.2. *Effect of the Expansion Ratio on Aerodynamic of the Flow behind the Step.* Obviously, in addition to the Reynolds number Re_s and boundary-layer thickness δ, the separated flow structure, friction, and separation-region length are affected by the channel-expansion ratio ER. The character of its influence on friction can be estimated by comparing the data in Fig. 4. The dashed curves show the friction coefficient corresponding to a steady laminar flow behind the flow-reattachment point. In other words, these values are obtained if the velocity profile is independent of the streamwise coordinate, and the boundary layers on the upper and lower walls of the channel merge and have an identical thickness. It follows from Fig. 4 that these lines are lower than the curves corresponding to various initial boundary-layer thicknesses. Hence, in all cases considered, the flow is not yet steady, which is caused by a comparatively small channel length.

For $ER = 1.17$ and 1.33, the behavior of the friction coefficient corresponds to that described in Sec. 3.1: its maximum absolute value in the separation region increases with decreasing initial boundary-layer thickness. At the same time, it follows from Fig. 4c that the maximum absolute value of the friction coefficient in the separation region is reached with increasing initial boundary-layer thickness for relatively narrow channels ($ER = 2.0$). This behavior, obviously, is explained by the close distance between the upper and lower walls of the channel, which is comparable with the step height. Convergence of the channel walls promotes a greater effect of the vortex from the recirculation region on the main flow.

The expansion ratio also affects the dependence of the separation-region length on the Reynolds number and initial boundary-layer thickness. Figure 6 shows the dependence $r(\mathrm{Re}_s)$ for $\delta = 0.24$ and expansion ratios

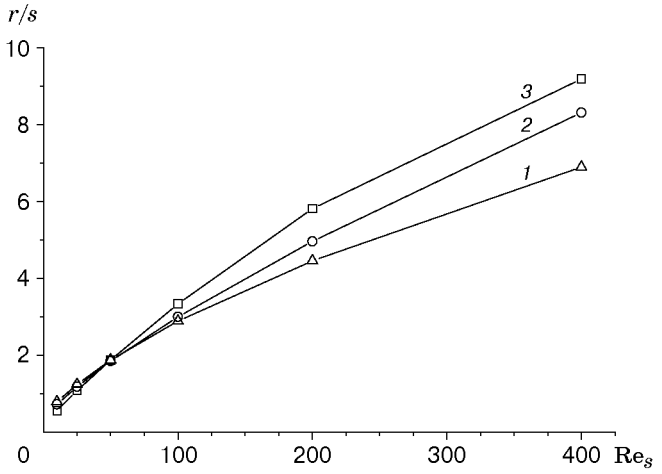

Fig. 6. Separation-region length r as a function of the Reynolds number Re_s for $\delta = 0.24$ and $ER = 1.17$ (1), 1.33 (2), and 2 (3).

$ER = 1.17$, 1.33, and 2.0 corresponding to $h = 6$, 3, and 1. It follows from Fig. 6 that the dependence $r(\mathrm{Re}_s)$ is close to linear for all values of ER considered. At the same time, with increasing ER, the slope of the curves in the most part of the examined range of Re_s increases, whereas the opposite trend is observed for $\mathrm{Re}_s < 50$, though the difference in r is not large. This behavior of the curves is, apparently, caused by two reasons. First, with increasing parameter ER, the relative thickness of the initial boundary layer with $\delta = \mathrm{const}$ increases. At the same time, the above results lead to an unambiguous conclusion: the greater the initial boundary-layer thickness, the greater the separation-region length. Second, the small distance between the upper and lower walls of the channel increases the influence of the vortex on flow parameters.

Conclusions. A steady laminar separated flow in a plane-parallel channel behind a rectangular backward-facing step is numerically simulated. It is shown that the dynamic prehistory of the flow and channel-expansion ratio exert a significant effect on the separation-region length and friction inside the latter. As the initial boundary-layer thickness decreases, the thickness of the shear layer in the separation region decreases, which, in turn, increases the friction coefficient and significantly decreases the separation-region length. An increase in the channel-expansion ratio with a fixed initial boundary-layer thickness leads to an increase in the separation-region length, which is caused by an increase in the relative thickness of the initial boundary layer.

The authors are grateful to N. I. Yarygina for valuable advice and comments.

This work was supported by the Russian Foundation for Fundamental Research (Grant No. 01-02-16842a).

REFERENCES

1. R. J. Goldstein, V. L. Eriksen, R. M. Olson, and E. R. G. Eckert, "Laminar separation, reattachment, and transition of the flow over a backward-facing step," *Teor. Osn. Inzh. Rasch.*, No. 4, 56–66 (1970).
2. K. R. Cramer, "On laminar separation bubbles," *J. Aeronaut. Sci.*, **25**, 143–144 (1958).
3. S. N. Sinha, A. K. Gupta, and M. M. Oberai, "Laminar separated flow around steps and cavities. 1. Flow behind a step," *AIAA J.*, **19**, No. 12, 1527–1530 (1981).
4. B. F. Armaly, F. Durst, J. C. F. Pereira, and B. Schonung, "Experimental and theoretical investigation of backward-facing step flow," *J. Fluid Mech.*, **127**, 473–496 (1983).
5. W. Aung, "An experimental study of Laminar heat transfer downstream of backsteps," *Teploperedacha*, **105**, No. 4, 143–149 (1983).
6. W. Aung, A. Baron, and F.-K. Tsou, "Wall independency and effect of initial shear-layer thickness in separated flow and heat transfer," *Int. J. Heat Mass Transfer*, **28**, No. 9, 1757–1770 (1985).
7. P. J. Roache, *Computational Fluid Mechanics*, Hermosa, Albuquerque (1976).
8. L. G. Leal and A. Acrivos, "The effect of base bleed on the steady separated flow past bluff objects," *J. Fluid Mech.*, **39**, 735–752 (1969).
9. T. J. Mueller and R. A. O'Leary, "Physical and numerical experiments in laminar incompressible separating and reattaching flow," AIAA Paper No. 70-763 (1970).